Noname manuscript No.
(will be inserted by the editor)

On the Estimation of Primary User Activity Statistics for Long and Short Time Scale Models in Cognitive Radio

Dhaval K. Patel · Brijesh Soni · Miguel López-Benítez

Manuscript received on February 28, 2019, revised on June 05, 2019.

Abstract Dynamic Spectrum Access (DSA)/Cognitive Radio (CR) systems access the channel in an opportunistic, non-interfering manner with the primary network. DSA/CR systems utilize spectrum sensing techniques to sense the availability of Primary user (PU). CR users can benefit from the knowledge of PU activity statistics. In this work, comprehensive analysis of estimation of distribution of PU idle and busy periods is carried out using Generalized Pareto and Pareto distributions for long and short time scale models respectively and closed form expression is derived. Moreover, the impact of sensing periods on the accuracy of estimated PU idle/busy periods is studied. Furthermore, the error in proposed estimation of distribution of PU idle and busy periods is quantified using the Kolmogorov-Smirnov test. From this study we conclude that the proposed model is better fit for the real scenarios eliminating practical limitations. Mathematical analysis is substantiated with the simulation results.

Keywords Dynamic spectrum access · Cognitive radio · Spectrum sensing · Generalized Pareto distribution · Primary user activity statistics.

1 Introduction

With the rapid development of wireless communications technology and the advent of 5G massive MIMO, spectrum resources are becoming highly scarce [1]. According to a spectrum occupancy campaign in 2016, the overall usage of the spectrum band ranges from 7% to 34%, which is quite poor [2]. The spectrum allocation needs to be dynamic for efficient usage and opportunistic access of the spectrum band. Digital Spectrum Access (DSA)/ Cognitive Radio (CR) systems is envisaged to be a reliable approach to solve this problem [3]. CR systems are classified in the literature as interweave, overlay and underlay paradigms. In interweave paradigms, which is the focus of this work, the secondary users (SUs) are not allowed to transmit during the activity of primary user (PU). On the otherhand, in underlay and overlay paradigms, simultaneous transmissions are allowed under the interference constraints.

DSA/CR system aims at increasing the spectral efficiency by allowing unlicensed or secondary users (SUs) to opportunistically access licensed spectrum bands temporarily unused by the licensed or primary users (PUs) in a non-interfering manner [4]. More specifically, CR exploits the parts of radio spectrum that are not occupied at some specific time instances in some specific locations and moves its operation to these parts called *spectrum holes or white spaces* for opportunistic access by spectrum sensing [5], [6]. Spectrum sensing decisions can be utilized by CR users to obtain information on PU channel activity. SU sense the PU channel periodically to decide the channel state (idle or busy) at every sensing event based on a signal detection algorithm [5], [7]. These spectrum decisions can be used to estimate the idle/busy time duration of the PU.

Once spectrum sensing is carried and opportunity of white space/ spectrum hole is found, channel prediction becomes an important aspect of DSA/CR systems. CR's can learn from their past observations, can pre-

Dhaval K. Patel, Brijesh Soni
School of Engineering and Applied Science, Ahmedabad University, India. E-mail: {dhaval.patel, brijesh.soni}@ahduni.edu.in

Miguel López-Benítez
Department of Electrical Engineering and Electronics, University of Liverpool, United Kingdom.
ARIES Research Centre, Antonio de Nebrija University, Madrid, Spain. E-mail: M.Lopez-Benitez@liverpool.ac.uk

dict and exploit the best channel from the pool of channels. Primary user activities also affect the channel prediction. There are many works in the literature where the channel prediction based on PU activity has been studied. Authors in [8] focuses on predicting the primary user channel activity using learning based hidden Markov model (HMM) for dynamic spectrum access, [9] studies the effect of PU activity on channel predictability. Also, the scenario becomes realistic when multiple users are present. Authors in [10] have provided a comprehensive study of orthogonal channel sets to the multiple users.

For a SU to opportunistically access a licensed spectrum band, it is important to have the knowledge of PU availability. The availability of the spectrum band can be estimated based on the PU's activity statistics (idle/busy periods, duty cycle etc.). Numerous work has been carried out in literature dealing with the statistics of idle/busy periods. For instance, the distribution of idle periods of PU is approximated using hyper-exponential density functions in [11]. Detailed analytical study of PU traffic classification using gamma and exponential distribution was carried out in [12]. Furthermore, unconstrained general idle time distribution of PU under imperfect sensing of SU and imperfect collision was studied in [13]. In a recent past, the comprehensive study of machine learning based prediction of PU activity statistics was carried out for CR systems in [14].

An investigation of how the statistical distribution of PU activity pattern in the time domain affects the ability of the CR system to obtain accurate statistical information based on spectrum sensing observations was carried out in [15]. This investigation proved that different occupancy patterns provide different accuracy levels. An analytical study relating the sensing period with the observed spectrum occupancy was carried out in [16]. The distributions of idle and busy periods were estimated considering the exponential distribution. Moreover, an accurate estimation of PU traffic based on periodic spectrum sensing was studied in [17]. Furthermore, an improved PU statistics prediction under imperfect spectrum sensing was carried out in [18].

Analytical study of estimating the PU idle and busy state holding times considering an exponential distribution was carried out in [16]. However, exponential distribution is a very specialized case and applies to certain specific scenarios. In [19], an empirical measurement study was carried out for various spectrum bands. In particular, long and short time scale measurements were carried out using spectrum analyzer and USRP respectively. As per [19], it was empirically proven that idle and busy states of PU over most of the spectrum bands is Generalized Pareto (and Pareto), which are considered as the best fit for long and short time scale measurements.

To the best of the authors' knowledge, no work in the literature has considered the estimation of PU activity statistics using the Generalized pareto and Pareto distribution, which is more realistic and empirically proven. In this context, our contribution in this article are threefold and can be summarized as follows:

- Firstly, an analytical study on the estimation of distribution of duration of PU idle and busy periods is carried out for long and short time scale models using Generalized Pareto and Pareto distributions as opposed to [16] in which exponential distribution is considered .
- Secondly, the impact of sensing periods on the accuracy of estimated PU idle/busy periods is studied.
- Thirdly, an error in the proposed estimation of distribution of PU idle and busy periods is quantified using the Kolmogorov-Smirnov (KS) goodness of fit test.

The rest of the paper is organized as follows. Section 2 describes the problem formulation of the PU channel activity statistics based on spectrum sensing. Section 3 analyses the estimation of long time scale model using Generalized Pareto distribution and estimates the error using KS distance. Section 4 analyses the estimation of short time scale model using Pareto distribution along with the analysis of estimation error using KS distance. Numerical results are discussed in section 5. Section 6 derives conclusion from the paper followed by Appendices.

2 Problem Formulation

Consider that SU detects PU based on the following alternating states as shown in Fig. 1. The idle/busy time duration of the PU can be estimated based on the sequence of the above stated binary alternating states.

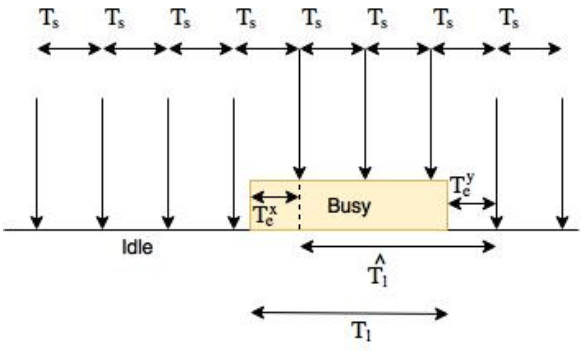

Fig. 1: Estimation of idle and busy periods.

Let T_s denote the periodic sensing duration, T_i denote the original period duration, where T_0 represents the time duration for which the PU was idle and T_1 represent the time duration for which the PU was busy. Similarly, let $\hat{T}_i$ denote the estimated period duration, where $\hat{T}_0$ represents the estimated time duration for which the PU was idle and $\hat{T}_1$ represent the estimated time duration for which the PU was busy. Here, T_e^x and T_e^y represent the error components encountered in the starting and ending estimated time durations as shown in Fig. 1 For the ease of analysis, we assume that the considered model in Fig. 1 is stationary. The concept of stationarity is relative, since a non-stationary process may be seen as "discretely stationary" when looked over a sufficiently short time interval such that it is nearly stationary in each observation interval, even though it may change from one observation interval to the next one. This is the reason why this work considers models at both long and short time scales and provides a separate analysis for each case. Even if the true distribution is not stationary, these models and the results presented in this work are still valid by considering that the distribution type is the same (e.g., Generalised Pareto, which is a more generic model and for which the Pareto distribution is a particular case) but the parameters of the distribution change over time. Such type of model was indeed proposed in Section IX of reference [19] (Two-Layer Modeling Approaches), where the use of the Pareto and Generalised Pareto models was justified based on results from empirical measurements. Further we assume that the idle and busy period follows the same distribution. Although the distribution is never stationary and it keeps evolving as per users' activity, the parameters of distribution vary over time (for both short and long time scale models considered).

Here, we assume high signal to noise ratio (SNR) scenarios with no sensing errors so that the only degrading effect of concern is the sensing duration, T_s. Ideally, the PU activity periods should be sensed accurately at the time of PU state change (i.e. from idle to busy or vice versa). However, in practice, the sensing of the PU state change is de-synchronised with sensing duration, T_s as shown in Fig. 1. Thus the estimated busy time duration can be written as follows :

$$\hat{T}_i = T_i + T_e \tag{1}$$

where $T_e = T_e^y - T_e^x$, denotes the error encountered in the estimation of busy duration of PU. Hence, the estimated duration, $\hat{T}_i$ not only depends on the original busy duration T_i, but also on the sensing duration, T_s. The main objective of this work is to derive closed form expressions of probability density function (PDF) and cumulative distribution function (CDF) of $\hat{T}_i$ as s function of T_i and T_s.

The error components T_e^x and T_e^y lie in the range (0, T_s) which can be appreciated from Fig. 1. Let both the error components, T_e^x and T_e^y follow uniform distribution (i.e. T_e^x and $T_e^y \sim U(0,T_s)$) [16].
Now, since $T_e = T_e^y - T_e^x$ the PDF of combined error T_e can be obtained by the convolution of distributions of $T_e^y \sim U(0,T_s)$ and $-T_e^x \sim U(-T_s,0)$ [20].

$$f_{T_e}(t) = f_{T_e^y}(t) * f_{-T_e^x}(t) = \int_{-\infty}^{\infty} f_{T_e^y}(\tau) f_{-T_e^x}(t-\tau)\mathrm{d}\tau \tag{2}$$

The '$*$' operator indicates the convolution operation. The convolution of two uniform distributions leads to a symmetric triangular distribution with width $2T_s$, $T_e \sim \Delta(-T_s, T_s)$.

The PDF of combined error T_e is as follows :

$$f_{T_e}(t) = \begin{cases} 0, & t < -T_s \\ \frac{T_s+t}{T_s^2}, & -T_s \le t < 0 \\ \frac{T_s-t}{T_s^2}, & 0 \le t \le T_s \\ 0, & t > T_s \end{cases} \tag{3}$$

Refer Section 8, Appendix 1 ■

3 Analysis of Long Time Scale Model

3.1 Estimation of Idle and Busy Periods Using Generalized Pareto distribution

Empirical test bed based spectrum measurement study carried out in [19] proved that long time scale measurements precisely follow Generalized Pareto distribution. In this analysis, we consider that the PU's idle and busy periods (i.e. T_0 and T_1) are assumed to be independent. The detailed study of correlation between the distributions of idle and busy periods was carried out in [21]. The correlation was quantified using Pearson, Kendall and Spearman correlation co-efficient. Findings in [21] suggest that the coefficient although not zero, is very low and thus not tightly correlated. Generalized Pareto distribution is a very generic case and highly reliable to real life scenarios than any other distribution such as exponential, Gamma etc. [19].

The PDF and CDF of Generalized Pareto distribution can be written as [22].

$$f_{T_i}(t) = \begin{cases} 0, & t < \mu \\ \frac{(\sigma)^{\frac{1}{\xi}}}{\left(\sigma+\xi(t-\mu)\right)^{\frac{1}{\xi}+1}}, & t \ge \mu \end{cases} \tag{4}$$

$$f_{\hat{T}_i}(t) = \begin{cases} 0, & t < \mu - T_s \\ \frac{(T_s+t-\mu)}{T_s^2} - \frac{1}{(1-\xi)(T_s^2)}\left[\sigma - (\sigma+\xi(t+T_s-\mu))^2 f_{T_i}(t+T_s)\right], & \mu - T_s \le t < \mu \\ \frac{T_s-t+\mu}{T_s^2} + \frac{1}{(1-\xi)(T_s^2)}\left[\sigma - 2(\sigma+\xi(t-\mu))^2 f_{T_i}(t) + (\sigma+\xi(t+T_s-\mu))^2 f_{T_i}(t+T_s)\right], & \mu \le t \le \mu + T_s \\ \frac{1}{(1-\xi)T_s^2}\left[(\sigma+\xi(t+T_s-\mu))^2 f_{T_i}(t+T_s) + (\sigma+\xi(t-T_s-\mu))^2 f_{T_i}(t-T_s) - 2(\sigma+\xi(t-\mu))^2 f_{T_i}(t)\right], & t > \mu + T_s \end{cases} \quad (5)$$

Refer Section 9, Appendix 2 ■

$$F_{\hat{T}_i}(t) = \begin{cases} 0, & t < \mu - T_s \\ \frac{T_s t + \frac{t^2}{2} - \mu t - \mu T_s + \frac{T_s^2}{2} + \frac{\mu^2}{2}}{T_s^2} - \frac{\sigma(t-\mu+T_s)}{(1-\xi)T_s^2} + \frac{(\sigma)^{\frac{1}{\xi}}}{(2\xi-1)(1-\xi)T_s^2}\left[(\sigma+\xi(t+T_s-\mu))^{2-\frac{1}{\xi}} - (\sigma)^{2-\frac{1}{\xi}}\right], & \mu - T_s \le t < \mu \\ \frac{1}{2} + \frac{(\sigma)(t-T_s-\mu)}{(1-\xi)T_s^2} - \frac{\mu-t}{T_s} - \frac{(\mu-t)^2}{2T_s^2} + \frac{(\sigma)^{\frac{1}{\xi}}}{(2\xi-1)(1-\xi)(T_s^2)}\left[(\sigma)^{2-\frac{1}{\xi}} + (\sigma+\xi(t+T_s-\mu))^{2-\frac{1}{\xi}} - 2(\sigma+\xi(t-\mu))^{2-\frac{1}{\xi}}\right], & \mu \le t \le \mu + T_s \\ 1 + \frac{(\sigma)^{\frac{1}{\xi}}}{(2\xi-1)(1-\xi)(T_s^2)}\left[(\sigma+\xi(t+T_s-\mu))^{2-\frac{1}{\xi}} - 2(\sigma+\xi(t-\mu))^{2-\frac{1}{\xi}} + (\sigma+\xi(t-T_s-\mu))^{2-\frac{1}{\xi}}\right], & t > \mu + T_s \end{cases} \quad (6)$$

Refer Section 10, Appendix 3 ■

$$F_{T_i}(t) = \begin{cases} 0, & t < \mu \\ 1 - \left(1 + \frac{\xi(t-\mu)}{\sigma}\right)^{-\frac{1}{\xi}}, & t \ge \mu \end{cases} \quad (7)$$

where, μ, σ and ξ are the distribution's location, scale and shape parameters respectively.

Since $\hat{T}_i = T_i + T_e$, the PDF of estimated periods can be written as a convolution of two distribution, obtained in similar way as (2),

$$f_{\hat{T}_i}(t) = f_{T_i}(t) * f_{T_e}(t) = \int_{-\infty}^{\infty} f_{T_i}(\tau) f_{T_e}(t-\tau)\mathrm{d}\tau$$

The resulting expression for PDF of estimated periods, $f_{\hat{T}_i}(t)$ is as shown in (5). Moreover, the CDF of the estimated periods, $F_{\hat{T}_i}(t)$ can be obtained from the PDF of estimated periods $f_{\hat{T}_i}(t)$ as follows [20]:

$$F_{\hat{T}_i}(t) = \int_{-\infty}^{t} f_{\hat{T}_i}(t)\mathrm{d}t \quad (8)$$

The resulting expression for CDF of estimated periods, $F_{\hat{T}_i}(t)$ is shown in (6). It can be noted that PDF and CDF of estimated periods hold different distributions for different range of values of time(t) which is due to the convolution of PDF of original and error components (similar for CDF). The significance of these 4 different cases lies in the fact that the estimated periods depend not only on original PU channel activity period duration, but also on sensing duration (T_s). Hence, the idle/busy periods of PU may lie in any range of the 4 possible ranges as shown in (5) and (6). Now, the PDFs and CDFs obtained in (5) and (6) have a continuous domain, while the actual distributions at the Secondary User have a discrete domain as indicated in Fig. 1. Such discrete distributions can be obtained by evaluating (5) and (6) at the right points of each interval/bin of the PDF and CDF, respectively as

$$g_{\hat{T}_i}(k) = f_{\hat{T}_i}(kT_s), \quad (9)$$

$$G_{\hat{T}_i}(k) = F_{\hat{T}_i}\left(\left(k + \frac{1}{2}\right)T_s\right), \quad (10)$$

where $g(.)$ and $G(.)$ denotes the estimated PDF and CDF respectively in the discrete domain and k is the integer value. The set of expressions derived above in (9) and (10) provide closed-form relations between the distributions of the original periods T_i resulting from PU transmission, the distribution of the estimated periods $\hat{T}_i$ as observed by the SU based on spectrum sensing decisions and the employed sensing duration, T_s.

3.2 Error of the Estimated Distribution

In this section, we quantify the error between the original distribution and the estimated distribution of idle/busy periods. Error of the estimated distribution can be calculated using KS test, a non-parametric test which is a well-known and most commonly used metric to quantify error between two distributions. The KS distance is defined as the largest absolute error between two continuous CDFs and given as follows [23] :

$$D_{ks} = \sup_t |F_{\hat{T}_i}(t) - F_{T_i}(t)|. \quad (11)$$

$$f_{\hat{T}_i}(t) = \begin{cases} 0, & t < \mu - T_s \\ \frac{\lambda\left(\frac{\lambda+t+T_s-\mu}{\lambda}\right)^{1-\alpha}+(\alpha-1)(t+T_s-\mu)-\lambda}{(\alpha-1)T_s^2}, & \mu - T_s \le t < \mu \\ \frac{\lambda}{T_s^2(\lambda-\alpha\lambda)}\Bigg[\left(\frac{\lambda+t-\mu}{\lambda}\right)^{-\alpha}((\alpha-1)T_s+\lambda+t-\mu)+\left(\frac{\lambda+t-\mu}{\lambda}\right)^{-\alpha}(-\alpha T_s+\lambda+t+T_s-\mu) \\ \quad -(\lambda+t+T_s-\mu)\left(\frac{\lambda+t+T_s-\mu}{\lambda}\right)^{-\alpha}+(\alpha-1)(t-T_s-\mu)-\lambda\Bigg], & \mu \le t \le \mu+T_s \\ \frac{1}{T_s^2(\lambda-\alpha\lambda)}\Bigg[-\lambda^2\left(\frac{\lambda+t+T_s-\mu}{\lambda}\right)^{1-\alpha}-\lambda\left(\lambda\left(\frac{\lambda+t-T_s-\mu}{\lambda}\right)^{1-\alpha}-\left(\frac{\lambda+t-\mu}{\lambda}\right)^{-\alpha}((\alpha-1)T_s+\lambda+t-\mu)\right) \\ \quad +\lambda\left(\frac{\lambda+t-\mu}{\lambda}\right)^{-\alpha}(-\alpha T_s+\lambda+t+T_s-\mu)\Bigg], & t > \mu+T_s \end{cases} \tag{12}$$

Refer section 11, Appendix 4 ■

$$F_{\hat{T}_i}(t) = \begin{cases} 0\ , & t < \mu - T_s \\ \frac{1}{2(\alpha-1)T_s^2}\left[\frac{2\lambda\left(\lambda\left(\frac{\lambda+t+T_s-\mu}{\lambda}\right)^{2-\alpha}-\lambda\right)}{2-\alpha}+(t+T_s-\mu)((\alpha-1)(t+T_s-\mu)-2\lambda)\right]\ , & \mu - T_s \le t < \mu \\ \frac{1}{2(\alpha-1)T_s^2}\left[\frac{2\lambda\left(\lambda\left(\frac{\lambda+T_s}{\lambda}\right)^{2-\alpha}-\lambda\right)}{2-\alpha}+T_s((\alpha-1)T_s-2\lambda)\right]-\frac{1}{(\alpha-1)T_s^2}\Bigg[-\frac{\lambda^2\left(\left(\frac{\lambda+T_s}{\lambda}\right)^{-\alpha}-2\right)}{\alpha-2} \\ \quad +\frac{\lambda\left(\frac{\lambda+t-\mu}{\lambda}\right)^{1-\alpha}(\alpha T_s-\lambda-t-2T_s+\mu)}{\alpha-2}-\frac{\lambda\left(\frac{\lambda+t-\mu}{\lambda}\right)^{1-\alpha}(\alpha T_s+\lambda+t-2T_s-\mu)}{\alpha-2}+\frac{(\lambda+t+T_s-\mu)^2\left(\frac{\lambda+t+T_s-\mu}{\lambda}\right)^{-\alpha}}{\alpha-2}+\frac{T_s^2\left(\frac{\lambda+T_s}{\lambda}\right)^{-\alpha}}{2-\alpha} \\ \quad +\lambda\left(\mu-\frac{2T_s\left(\frac{\lambda+T_s}{\lambda}\right)^{-\alpha}}{\alpha-2}\right)+\frac{\alpha t^2}{2}-\alpha t T_s-\alpha t\mu+(\alpha-1)T_s\mu+\frac{1}{2}(\alpha-1)\mu^2-\lambda t-\frac{t^2}{2}+tT_s+t\mu\Bigg]\ , & \mu \le t \le \mu+T_s \\ \frac{1}{2(2-\alpha)(\alpha-1)^2T_s^2}\Bigg[2T_s^2\Bigg(-\left(\frac{\lambda+t-T_s-\mu}{\lambda}\right)^{-\alpha}-\left(\frac{\lambda+t+T_s-\mu}{\lambda}\right)^{-\alpha}+\alpha\Bigg(\left(\frac{\lambda+t-T_s-\mu}{\lambda}\right)^{-\alpha}+\left(\frac{\lambda+t+T_s-\mu}{\lambda}\right)^{-\alpha} \\ \quad -(\alpha-4)\alpha-5\Bigg)+2\Bigg)+4(\alpha-1)T_s(\lambda+t-\mu)\left(\left(\frac{\lambda+t+T_s-\mu}{\lambda}\right)^{-\alpha}-\left(\frac{\lambda+t-T_s-\mu}{\lambda}\right)^{-\alpha}\right) \\ \quad +2(\alpha-1)(\lambda+t-\mu)^2\left(\left(\frac{\lambda+t-T_s-\mu}{\lambda}\right)^{-\alpha}+\left(\frac{\lambda+t+T_s-\mu}{l}\right)^{-\alpha}-2\left(\frac{\lambda+t-\mu}{\lambda}\right)^{-\alpha}\right)\Bigg]\ , & t > \mu+T_s \end{cases} \tag{13}$$

Refer section 12, Appendix 5 ■

In order to find the value of 't' that returns the maximum value of KS Distance from (11), the partial derivative of the absolute difference is taken and equated to zero as follows :

$$\frac{\partial[F_{\hat{T}_i}(t) - F_{T_i}(t)]}{\partial t} = 0. \tag{14}$$

On evaluating (18), the largest difference occurs at t = μ, where $F_{T_i}(t) = 0$. Hence, the final expression for KS distance will be

$$D_{ks} = F_{\hat{T}_i}(t) = \frac{1}{2} - \frac{\sigma}{(1-\xi)(T_s)} - \frac{\sigma^2}{(2\xi-1)(1-\xi)(T_s^2)} + \frac{\sigma^{\frac{1}{\xi}}(\sigma+\xi T_s)^{2-\frac{1}{\xi}}}{(2\xi-1)(1-\xi)(T_s^2)} \tag{15}$$

Equation (15) denotes the expression for calculating the KS distance between the estimated and original distributions. Conversely, the value of T_s can be calculated on setting the target error in (15).

4 Analysis of Short Time Scale Model

4.1 Estimation of Idle and Busy Periods Using Pareto Distribution

In this section, we estimate the distribution of idle and busy periods of short time scale model as Pareto distribution. For simplicity, the PU's idle and busy periods (i.e. T_0 and T_1) are assumed to be independent. Pareto distribution is empirically proven efficient distribution for the spectrum measurements using USRP [19]. The PDF and CDF of Pareto distribution is given as [22],

$$f_{T_i}(t) = \begin{cases} 0, & t < \mu \\ \frac{\alpha}{\lambda}\left(1+\frac{t-\mu}{\lambda}\right)^{-(\alpha+1)}, & t \ge \mu \end{cases} \tag{16}$$

$$F_{T_i}(t) = \begin{cases} 0, & t < \mu \\ 1-\left(1+\frac{t-\mu}{\lambda}\right)^{-\alpha}, & t \ge \mu \end{cases} \tag{17}$$

where α, λ and μ are the shape, scale and location parameters respectively. The estimated periods can be

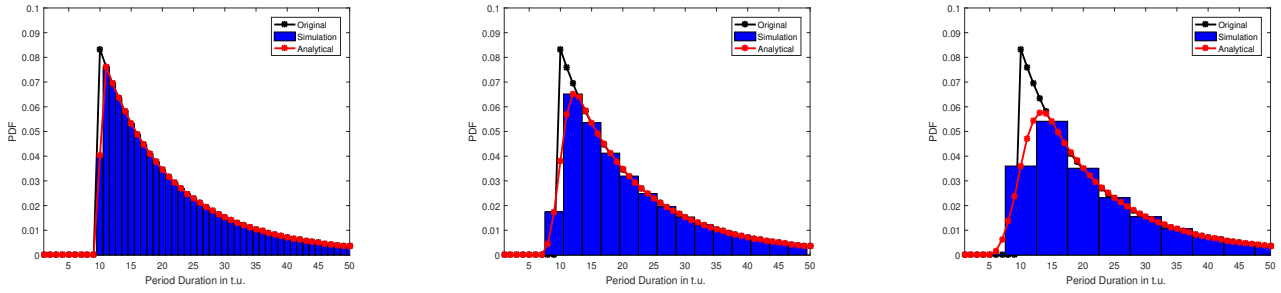

((a)) T_s = 1 t.u ((b)) T_s = 3 t.u ((c)) T_s = 5 t.u

Fig. 2: Validation of PDF of estimated periods for Generalized Pareto distribution using ($\mu = 10, \sigma = 12, \xi = 0.1$)

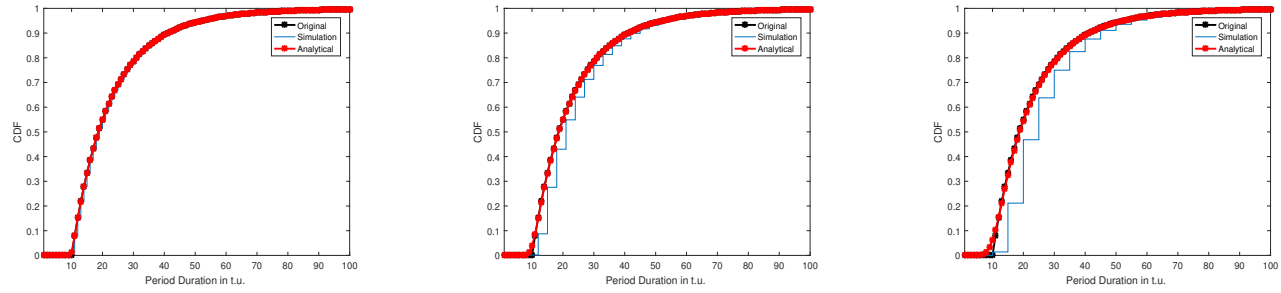

((a)) T_s = 1 t.u ((b)) T_s = 3 t.u ((c)) T_s = 5 t.u

Fig. 3: Validation of CDF of estimated periods for Generalized Pareto distribution using ($\mu = 10, \sigma = 12, \xi = 0.1$)

written as

$$f_{\hat{T}_i}(t) = f_{T_i}(t) * f_{T_e}(t) = \int_{-\infty}^{\infty} f_{T_i}(\tau) f_{T_e}(t-\tau) \mathrm{d}\tau,$$

where $f_{T_i}(\tau)$ and $f_{T_e}(t-\tau)$ are the PDF of Pareto distribution and error component respectively. On further evaluating the integral in the four intervals/cases as mentioned earlier and on solving in the similar lines as done for long time scale models and with the aid of [24] and [25], the estimated PDF and CDF of idle/busy periods for short time scale measurements can be obtained as (12) and (13) respectively. Refer appendices 4 and 5 for proof.

4.2 Error of the Estimated distribution

In this section the KS distance of the estimated idle and busy periods using Pareto distribution is computed in similar fashion as calculated in section 3.2. In order to find the value of 't' that returns the maximum value of KS Distance, the partial derivative of the absolute difference is taken and equated to zero as follows :

$$\frac{\partial[F_{\hat{T}_i}(t) - F_{T_i}(t)]}{\partial t} = 0 \tag{18}$$

On evaluating (18), we can observe from the CDF plot of Pareto distribution that the largest difference occurs at t = μ, where $F_{T_i}(t) = 0$. Hence, the final expression for KS distance will be:

$$\begin{aligned} D_{ks} = \frac{1}{2\left(\alpha^2 - 3\alpha + 2\right) T_s^2} \Bigg[& T_s^2 \left(\alpha^2 - 2 \left(\frac{\lambda + T_s}{\lambda} \right)^{-\alpha} - 3\alpha + 2 \right) \\ & + \lambda^2 \left(2 - 2 \left(\frac{\lambda + T_s}{\lambda} \right)^{-\alpha} \right) \\ & + 2\lambda T_s \left(-2 \left(\frac{\lambda + T_s}{\lambda} \right)^{-\alpha} - \alpha + 2 \right) \Bigg] \end{aligned} \tag{19}$$

Equation (19) denotes the expression for calculating the KS distance between the estimated and original distributions.

5 Numerical Results

In this section, we verify the accuracy of the closed form expressions of estimated PDF and CDF derived in Section 3 and 4 by comparing them with the original and simulated PDF and CDF distributions of PU. Further, we study effect of sensing time on the estimated distribution by considering the KS distance values for different values of sensing time, T_s. For simulation and analysis, idle and busy period are assumed to follow the same distribution (in respective time-scale models).

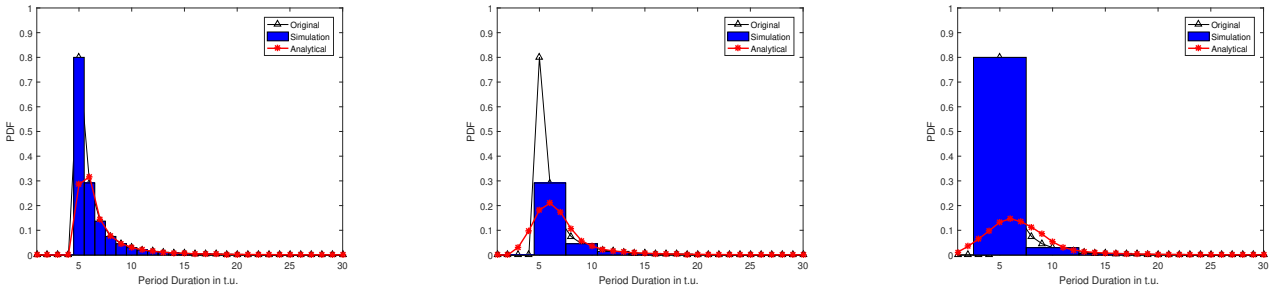

((a)) T_s = 1 t.u ((b)) T_s = 3 t.u ((c)) T_s = 5 t.u

Fig. 4: Validation of PDF of estimated periods for Pareto distribution using ($\mu = 5, \alpha = 2, \lambda = 2.5$)

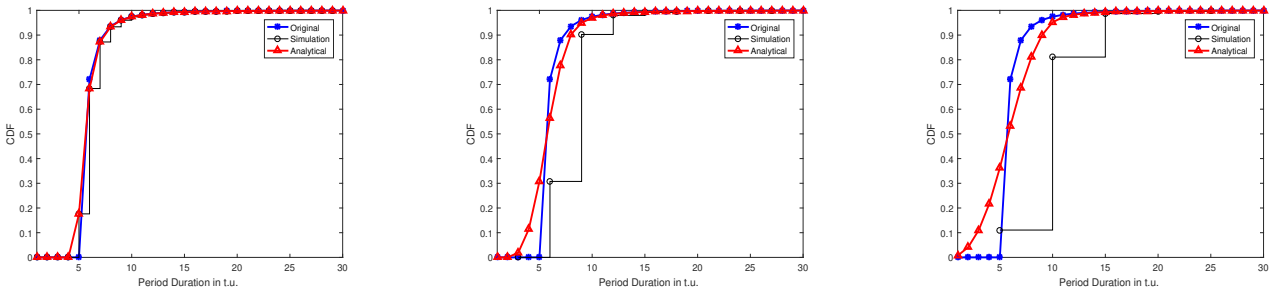

((a)) T_s = 1 t.u ((b)) T_s = 3 t.u ((c)) T_s = 5 t.u

Fig. 5: Validation of CDF of estimated periods for Pareto distribution($\mu = 5, \alpha = 2.5, \lambda = 1.5$)

For all the cases considered here, the value of sensing duration, T_s is configured such that it does not exceed the value of μ (i.e. $T_s < \mu$) in order to ensure that no activity periods are missed in the sensing process, since we are ignoring the effect of missed detections and false alarms in our analytical framework. Notice that this consideration implicitly assumes that the minimum PU activity is known to the SU, so that the value of sensing time, T_s can be configured as stated above. This assumption is realistic too, since the value of μ is available for some well-known standardized radio technologies or can also be obtained with methods such as blind recognition/estimation [26] or from PU beacon signals [27]. The idle and busy period were generated considering both to be independent. The comprehensive study in our previous work [21] suggest that the distribution has a very low value of Pearson-coefficient and thus can be considered independent.

Fig. 2 shows the PDF of estimated busy period $f_{\hat{T}_i}(t)$ of the PU, in comparison with the simulated busy period $g_{\hat{T}_i}(t)$ and the original distribution $f_{T_i}(t)$ for different values of T_s (i.e. T_s = 1, 3 and 5 time units). The parameters of the Generalized Pareto distribution are configured to values : μ = 10, σ = 12, ξ = 0.1. It can be appreciated that the closed form analysis provides an excellent fit with the simulation results for all the considered scenarios, which verifies the validity of the mathematical expression obtained for the PDF.

Fig. 3 shows the CDF of estimated busy period $F_{\hat{T}_i}(t)$ of the PU, in comparison with the simulated busy period $G_{\hat{T}_i}(t)$ and the original distribution $F_{T_i}(t)$ for different values of T_s (i.e. T_s = 1, 3 and 5 time units). The parameters of the Generalized Pareto distribution are configured to values : μ = 10, σ = 12, ξ = 0.1. We can notice the closed form analysis provides a good match with the simulation results for all the considered scenarios, which verifies the validity of the mathematical expression obtained for the CDF as well.

Fig. 4 and Fig. 5 shows the PDF and CDF of estimated busy period $f_{\hat{T}_i}(t)$ of PU, for Pareto distribution in comparison with the simulated busy period $g_{\hat{T}_i}(t)$ and the original distribution $f_{T_i}(t)$ for different sensing time duration, T_s (i.e. T_s = 1, 3 and 5 time units). The parameters of the Pareto distribution are : μ = 5, α = 2, λ = 2.5 for estimated PDF while μ = 5, α = 2.5, λ = 1.5 for estimated CDF. We observe that the closed form analysis provides an excellent fit with the simulation results for all the considered scenarios, which verifies the validity of the expression obtained for the PDF and CDF for short time scale model.

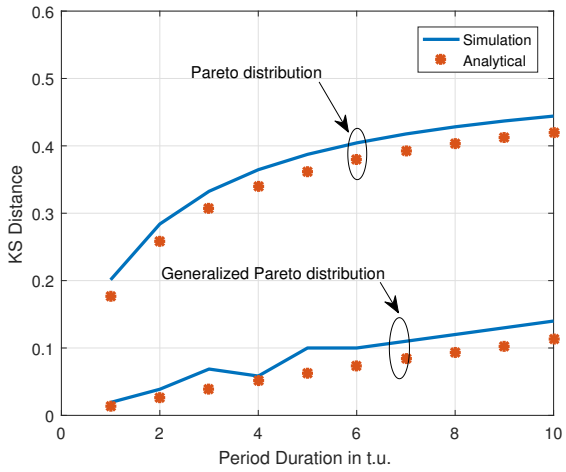

Fig. 6: Comparison of KS Distance for Pareto and Generalized Pareto distribution.

Fig. 6 shows the comparison of KS Distance v/s T_s for simulated and analytical CDF with respect to the original distribution for Generalized Pareto and Pareto distribution. As it can be appreciated from Fig. 6, the analytical expression in (15) and (19) gives a prediction of the estimation error for both the time scale models. Also, we observe that the values of errors becomes slightly large for larger values of sensing time duration, T_s. Hence, the desired value of estimation error can be achieved by configuring the sensing duration accordingly. We can observe that the estimated and original CDF are in good agreement for both the models.

In summary, we can conclude that the assumptions made in the study are reasonable from a practical point of view. The obtained results corroborate that they are acceptable since the simulation results and the mathematical models are accurate.

6 Conclusion

DSA/CR systems periodically monitor the PU channel activity statistics. Hence, the CR would highly benefit from the accurate knowledge of the derived analytical expressions for the PDF and CDF of the idle and busy time periods of the PU. From this study, we conclude that the analysis of estimation of distribution of PU idle and busy periods is carried out using Generalized Pareto and Pareto distributions for long and short time scale models provides an accurate fit with the original distribution, which are verified using simulations. Moreover, the impact of sensing periods on the accuracy of estimated PU busy/idle periods has also studied. Furthermore, an error in the proposed estimation of distribution of PU idle and busy periods is quantified using Kolmogorov-Smirnov test for Generalized Pareto and Pareto distribution. Our work can be seen as a study where we provide the "tool" i.e., the analytical expressions for the true and estimated distributions, and the resulting estimation error. the analytical expression can be useful in the design and dimensioning of CR networks. The current analysis can be extended by considering the imperfect spectrum sensing, which is further more realistic assumption and yet is to be reported in literature. Furthermore, the online learning of distributions of the idle and busy period would be an interesting study of prospective research. Moreover, the analysis carried in this work is for interweave CR paradigm. The comprehensive study considering the underlay and overlay paradigm, which includes the interference scenario is out of the scope of this work and will be addressed in our future work. From this study we conclude that the proposed analysis is more generic, is better fit for the real scenarios eliminating practical limitations and can be used in the design and development of CR systems.

7 Acknowledgement

This work is supported by Department of Science and Technology (DST)-UKIERI Programme under the Grant ref. DST/INT/UK/P-150/2016. The authors would like to thank School of Engineering and Applied Science, Ahmedabad University and the University of Liverpool, UK for the infrastructural support.

8 Appendix 1: Derivation of the combined error T_e

$$f_{T_e}(t) = f_{T_e^y}(t) * f_{-T_e^x}(t) = \int_{-\infty}^{\infty} f_{T_e^y}(\tau) f_{-T_e^x}(t-\tau)\mathrm{d}\tau \quad (20)$$

Case 1 : $t < -T_s$

No overlap in both the distributions, i.e. $f_{T_e^y}(\tau)$ and $f_{-T_e^x}(t-\tau)$.

$$\therefore \int_{-\infty}^{-T_s} f_{T_e^y}(\tau) f_{-T_e^x}(t-\tau)\mathrm{d}\tau = 0$$

Case 2 : $-T_s \leq t < 0$

$$\int_{-T_s}^{t} f_{T_e^y}(\tau) f_{-T_e^x}(t-\tau)\mathrm{d}\tau = \int_{-T_s}^{t} \left(\frac{1}{T_s}\right)\left(\frac{1}{T_s}\right)\mathrm{d}\tau = \frac{T_s + t}{T_s^2}$$

Case 3 : $0 \leq t \leq T_s$

$$\int_{t}^{T_s} f_{T_e^y}(\tau) f_{-T_e^x}(t-\tau)\mathrm{d}\tau = \int_{t}^{T_s} \left(\frac{1}{T_s}\right)\left(\frac{1}{T_s}\right)\mathrm{d}\tau = \frac{T_s - t}{T_s^2}$$

Case 4 : $t > T_s$

No overlap in both the distributions, i.e. $f_{T_e^y}(\tau)$ and $f_{-T_e^x}(t-\tau)$.

$$\therefore \int_{T_s}^{\infty} f_{T_e^y}(\tau) f_{-T_e^x}(t-\tau)\mathrm{d}\tau = 0$$

9 Appendix 2 : Derivation of PDF of estimated periods for Generalized Pareto Distribution

Case 1 : $t + T_s < \mu \implies t < \mu - T_s$

No overlap in both the distributions, i.e. $f_{T_i}(\tau)$ and $f_{T_e}(t-\tau)$.

$$f_{\hat{T}_i}(t) = \int_{-\infty}^{\mu - T_s} f_{T_i}(\tau) f_{T_e}(t-\tau)\mathrm{d}\tau = 0$$

Case 2 : $\mu - T_s \le t < \mu$

$$\begin{aligned} f_{\hat{T}_i}(t) &= \int_{\mu}^{t+T_s} \frac{(\sigma)^{\frac{1}{\xi}}}{\Big(\sigma + \xi(\tau-\mu)\Big)^{\frac{1}{\xi}+1}} \Big(\frac{T_s + t - \tau}{T_s^2}\Big)\mathrm{d}\tau \\ &= \frac{(\sigma)^{\frac{1}{\xi}}}{T_s^2}\Big[\int_{\mu}^{t+T_s} (T_s + t)\Big(\sigma + \xi(\tau-\mu)\Big)^{-\frac{1}{\xi}-1} \\ &\qquad - \int_{\mu}^{t+T_s} (\tau)\Big(\sigma + \xi(\tau-\mu)\Big)^{-\frac{1}{\xi}-1}\mathrm{d}\tau\Big] \end{aligned}$$

Solving both the above integrals separately and combining them, we get,

$$\begin{aligned} f_{\hat{T}_i}(t) &= \frac{(T_s + t - \mu)}{T_s^2} \\ &\quad - \frac{1}{(1-\xi)(T_s^2)}\Big[\sigma - (\sigma + \xi(t + T_s - \mu))^2 f_{T_i}(t + T_s)\Big] \end{aligned}$$

Case 3 : $\mu \le t \le \mu + T_s$

$$\begin{aligned} f_{\hat{T}_i}(t) &= \int_{\mu}^{t+T_s} f_{T_i}(\tau) f_{T_e}(t-\tau)\mathrm{d}\tau \\ &= \int_{\mu}^{t} \frac{(\sigma)^{\frac{1}{\xi}}}{\Big(\sigma + \xi(\tau-\mu)\Big)^{\frac{1}{\xi}+1}} \Big(\frac{T_s - t + \tau}{T_s^2}\Big)\mathrm{d}\tau \\ &\quad + \int_{t}^{t+T_s} \frac{(\sigma)^{\frac{1}{\xi}}}{\Big(\sigma + \xi(\tau-\mu)\Big)^{\frac{1}{\xi}+1}} \Big(\frac{T_s + t - \tau}{T_s^2}\Big)\mathrm{d}\tau \end{aligned}$$

Solving the above integrals separately and combining them, we get,

$$\begin{aligned} f_{\hat{T}_i}(t) &= \frac{T_s - t + \mu}{T_s^2} + \frac{1}{(1-\xi)(T_s^2)}\Big[\sigma - 2(\sigma + \xi(t-\mu))^2 f_{T_i}(t) \\ &\qquad + (\sigma + \xi(t + T_s - \mu))^2 f_{T_i}(t + T_s)\Big] \end{aligned}$$

Case 4 : $t > \mu + T_s$

$$\begin{aligned} f_{\hat{T}_i}(t) &= \int_{t-T_s}^{t+T_s} f_{T_i}(\tau) f_{T_e}(t-\tau)\mathrm{d}\tau \\ &= \int_{t-T_s}^{t} \frac{(\sigma)^{\frac{1}{\xi}}}{\Big(\sigma + \xi(\tau-\mu)\Big)^{\frac{1}{\xi}+1}} \Big(\frac{T_s - t + \tau}{T_s^2}\Big)\mathrm{d}\tau \\ &\quad + \int_{t}^{t+T_s} \frac{(\sigma)^{\frac{1}{\xi}}}{\Big(\sigma + \xi(\tau-\mu)\Big)^{\frac{1}{\xi}+1}} \Big(\frac{T_s + t - \tau}{T_s^2}\Big)\mathrm{d}\tau \end{aligned}$$

Solving the above two integrals and combining them, we get,

$$\begin{aligned} f_{\hat{T}_i}(t) &= \frac{1}{(1-\xi)T_s^2}\Big[(\sigma + \xi(t + T_s - \mu))^2 f_{T_i}(t + T_s) \\ &\qquad + (\sigma + \xi(t - T_s - \mu))^2 f_{T_i}(t - T_s) \\ &\qquad - 2(\sigma + \xi(t-\mu))^2 f_{T_i}(t)\Big] \end{aligned}$$

10 Appendix 3 : Derivation of CDF of estimated periods for Generalized Pareto Distribution

$$F_{\hat{T}_i}(t) = \int_{-\infty}^{t} f_{\hat{T}_i}(\tau)\mathrm{d}\tau \tag{21}$$

Case 1 : $t < \mu - T_s$

Substituting the PDF derived in Case 1 of Section 9, we get,

$$F_{\hat{T}_i}(t) = \int_{-\infty}^{t} 0\mathrm{d}\tau = 0$$

Case 2 : $\mu - T_s \le t < \mu$

$$F_{\hat{T}_i}(t) = \int_{-\infty}^{t} f_{\hat{T}_i}(\tau)\mathrm{d}\tau = \int_{-\infty}^{\mu - T_s} 0\mathrm{d}\tau + \int_{\mu - T_s}^{t} f_{T_i}(\tau)\mathrm{d}\tau$$

Solving the above integrals by substituting the appropriate PDFs derived for Case 1 and Case 2 in Section 9 and combining them, we get,

$$\begin{aligned} F_{\hat{T}_i}(t) &= \frac{1}{2} - \frac{(\mu - t)}{T_s} + \frac{(\mu - t)^2}{2T_s^2} - \frac{\sigma(t - \mu + T_s)}{(1-\xi)T_s^2} \\ &\quad + \frac{(\sigma)^{\frac{1}{\xi}}}{(2\xi - 1)(1-\xi)T_s^2}\Big[(\sigma + \xi(t + T_s - \mu))^{2-\frac{1}{\xi}} - (\sigma)^{2-\frac{1}{\xi}}\Big] \end{aligned}$$

Case 3 : $\mu \le t \le \mu + T_s$

$$F_{\hat{T}_i}(t) = \int_{-\infty}^{t} f_{\hat{T}_i}(\tau)\mathrm{d}\tau$$
$$= \int_{-\infty}^{\mu-T_s} 0\mathrm{d}\tau + \int_{\mu-T_s}^{\mu} f_{T_i}(\tau)\mathrm{d}\tau + \int_{\mu}^{t} f_{T_i}(\tau)\mathrm{d}\tau$$

Solving the above integrals by substituting the appropriate PDFs derived for Case 1, Case 2 and Case 3 in Section 9 and combining them, we get,

$$F_{\hat{T}_i}(t) = \frac{1}{2} - \frac{\mu - t}{T_s} - \frac{(\mu-t)^2}{2T_s^2} + \frac{(\sigma)(t-\mu-T_s)}{(1-\xi)T_s^2}$$
$$+ \frac{(\sigma)^{\frac{1}{\xi}}}{(2\xi-1)(1-\xi)(T_s^2)}\Big[(\sigma+\xi(t+T_s-\mu))^{2-\frac{1}{\xi}}$$
$$+ (\sigma)^{2-\frac{1}{\xi}} - 2(\sigma+\xi(t-\mu))^{2-\frac{1}{\xi}}\Big]$$

Case 4 : $t > \mu + T_s$

$$F_{\hat{T}_i}(t) = \int_{-\infty}^{t} f_{\hat{T}_i}(\tau)\mathrm{d}\tau$$
$$= \int_{-\infty}^{\mu-T_s} 0\mathrm{d}\tau + \int_{\mu-T_s}^{\mu} f_{T_i}(\tau)\mathrm{d}\tau$$
$$+ \int_{\mu}^{\mu+T_s} f_{T_i}(\tau)\mathrm{d}\tau + \int_{\mu+T_s}^{t} f_{T_i}(\tau)\mathrm{d}\tau$$

Solving the above integrals by substituting the appropriate PDFs derived for Case 1, Case 2, Case 3 and Case 4 in Section 9 and combining them, we get,

$$F_{\hat{T}_i}(t) = 1 + \frac{(\sigma)^{\frac{1}{\xi}}}{(2\xi-1)(1-\xi)(T_s^2)}\Big[(\sigma+\xi(t+T_s-\mu))^{2-\frac{1}{\xi}}$$
$$- 2(\sigma+\xi(t-\mu))^{2-\frac{1}{\xi}} + (\sigma+\xi(t-T_s-\mu))^{2-\frac{1}{\xi}}\Big]$$

11 Appendix 4 : Derivation of PDF of estimated periods for Pareto Distribution

Case 1 : $t + T_s < \mu \implies t < \mu - T_s$

No overlap in both the distributions, i.e. $f_{T_i}(\tau)$ and $f_{T_e}(t-\tau)$.

$$f_{\hat{T}_i}(t) = \int_{-\infty}^{\mu-T_s} f_{T_i}(\tau) f_{T_e}(t-\tau)\mathrm{d}\tau = 0$$

Case 2 : $\mu - T_s \le t < \mu$

$$f_{\hat{T}_i}(t) = \int_{\mu}^{t+T_s} \frac{\alpha}{\lambda}\left(1+\frac{t-\mu}{\lambda}\right)^{-(\alpha+1)}\left(\frac{T_s-t+\tau}{T_s^2}\right)d\tau$$

On solving the above integral, we get

$$f_{\hat{T}_i}(t) = \frac{\lambda\left(\frac{\lambda+t+T_s-\mu}{\lambda}\right)^{1-\alpha} + (\alpha-1)(t+T_s-\mu) - \lambda}{(\alpha-1)T_s^2}$$

Case 3 : $\mu \le t \le \mu + T_s$

$$f_{\hat{T}_i}(t) = \int_{\mu}^{t+T_s} f_{T_i}(\tau) f_{T_e}(t-\tau)\mathrm{d}\tau$$
$$= \int_{\mu}^{t} \frac{\alpha}{\lambda}\left(1+\frac{t-\mu}{\lambda}\right)^{-(\alpha+1)}\left(\frac{T_s-t+\tau}{T_s^2}\right)d\tau$$
$$+ \int_{t}^{t+T_s} \frac{\alpha}{\lambda}\left(1+\frac{t-\mu}{\lambda}\right)^{-(\alpha+1)}\left(\frac{T_s+t-\tau}{T_s^2}\right)d\tau$$

Solving the above integrals separately and combining them, we get,

$$f_{\hat{T}_i}(t) = \frac{\lambda}{T_s^2(\lambda-\alpha\lambda)}\Big[\left(\frac{\lambda+t-\mu}{\lambda}\right)^{-\alpha}((\alpha-1)T_s$$
$$+ \lambda + t - \mu) + \left(\frac{\lambda+t-\mu}{\lambda}\right)^{-\alpha}(-\alpha T_s + \lambda + t + T_s - \mu)$$
$$- (\lambda + t + T_s - \mu)\left(\frac{\lambda+t+T_s-\mu}{\lambda}\right)^{-\alpha}$$
$$+ (\alpha-1)(t-T_s-\mu) - \lambda\Big]$$

Case 4 : $t > \mu + T_s$

$$f_{\hat{T}_i}(t) = \int_{t-T_s}^{t+T_s} \frac{\alpha}{\lambda}\left(1+\frac{t-\mu}{\lambda}\right)^{-(\alpha+1)}\left(\frac{T_s-t+\tau}{T_s^2}\right)d\tau$$
$$+ \int_{t}^{t+T_s} \frac{\alpha}{\lambda}\left(1+\frac{t-\mu}{\lambda}\right)^{-(\alpha+1)}\left(\frac{T_s+t-\tau}{T_s^2}\right)d\tau$$

Solving the above two integrals and combining them, we get,

$$f_{\hat{T}_i}(t) = \frac{1}{T_s^2(\lambda-\alpha\lambda)}\Big[-\lambda^2\left(\frac{\lambda+t+T_s-\mu}{\lambda}\right)^{1-\alpha}$$
$$- \lambda\Big(\lambda\left(\frac{\lambda+t-T_s-\mu}{\lambda}\right)^{1-\alpha} - \left(\frac{\lambda+t-\mu}{\lambda}\right)^{-\alpha}$$
$$((\alpha-1)T_s + \lambda + t - \mu)\Big) + \lambda\left(\frac{\lambda+t-\mu}{\lambda}\right)^{-\alpha}$$
$$\times(-\alpha T_s + \lambda + t + T_s - \mu)\Big].$$

12 Appendix 5 : Derivation of CDF of estimated periods for Pareto Distribution

$$F_{\hat{T}_i}(t) = \int_{-\infty}^{t} f_{\hat{T}_i}(\tau)\mathrm{d}\tau \tag{22}$$

Case 1 : $t < \mu - T_s$

Substituting the PDF derived in Case 1 of Section 11, we get,

$$F_{\hat{T}_i}(t) = \int_{-\infty}^{t} 0\mathrm{d}\tau = 0$$

Case 2 : $\mu - T_s \leq t < \mu$

$$F_{\hat{T}_i}(t) = \int_{-\infty}^{t} f_{\hat{T}_i}(\tau)\mathrm{d}\tau = \int_{-\infty}^{\mu-T_s} 0\mathrm{d}\tau + \int_{\mu-T_s}^{t} f_{\hat{T}_i}(\tau)\mathrm{d}\tau$$

Solving the above integrals by substituting the appropriate PDFs derived for Case 1 and Case 2 in Section 11 and combining them, we get,

$$F_{\hat{T}_i}(t) = \frac{1}{2(\alpha-1)T_s^2}\left[\frac{2\lambda\left(\lambda\left(\frac{\lambda+t+T_s-\mu}{\lambda}\right)^{2-\alpha} - \lambda\right)}{2-\alpha} + (t+T_s-\mu)((\alpha-1)(t+T_s-\mu)-2\lambda)\right]$$

Case 3 : $\mu \leq t \leq \mu + T_s$

$$F_{\hat{T}_i}(t) = \int_{-\infty}^{t} f_{\hat{T}_i}(\tau)\mathrm{d}\tau = \int_{-\infty}^{\mu-T_s} 0\mathrm{d}\tau + \int_{\mu-T_s}^{\mu} f_{\hat{T}_i}(\tau)\mathrm{d}\tau + \int_{\mu}^{t} f_{\hat{T}_i}(\tau)\mathrm{d}\tau$$

Solving the above integrals by substituting the appropriate PDFs derived for Case 1, Case 2 and Case 3 in Section 11 and combining them, we get,

$$\begin{aligned}
F_{\hat{T}_i}(t) = \frac{1}{2(\alpha-1)T_s^2}\Bigg[&\frac{2\lambda\left(\lambda\left(\frac{\lambda+T_s}{\lambda}\right)^{2-\alpha} - \lambda\right)}{2-\alpha} + T_s((\alpha-1)T_s - 2\lambda)\Bigg] \\
&- \frac{1}{(\alpha-1)T_s^2}\Bigg[-\frac{\lambda^2\left(\left(\frac{\lambda+T_s}{\lambda}\right)^{-\alpha} - 2\right)}{\alpha-2} \\
&+ \frac{\lambda\left(\frac{\lambda+t-\mu}{\lambda}\right)^{1-\alpha}(\alpha T_s - \lambda - t - 2T_s + \mu)}{\alpha-2} \\
&- \frac{\lambda\left(\frac{\lambda+t-\mu}{\lambda}\right)^{1-\alpha}(\alpha T_s + \lambda + t - 2T_s - \mu)}{\alpha-2} \\
&+ \frac{(\lambda+t+T_s-\mu)^2\left(\frac{\lambda+t+T_s-\mu}{\lambda}\right)^{-\alpha}}{\alpha-2} + \frac{T_s^2\left(\frac{\lambda+T_s}{\lambda}\right)^{-\alpha}}{2-\alpha} \\
&+ \lambda\left(\mu - \frac{2T_s\left(\frac{\lambda+T_s}{\lambda}\right)^{-\alpha}}{\alpha-2}\right) + \frac{\alpha t^2}{2} - \alpha t T_s - \alpha t\mu \\
&+ (\alpha-1)T_s\mu + \frac{1}{2}(\alpha-1)\mu^2 - \lambda t - \frac{t^2}{2} + tT_s + t\mu\Bigg]
\end{aligned}$$

Case 4 : $t > \mu + T_s$

$$\begin{aligned}
F_{\hat{T}_i}(t) &= \int_{-\infty}^{t} f_{\hat{T}_i}(\tau)\mathrm{d}\tau \\
&= \int_{-\infty}^{\mu-T_s} 0\mathrm{d}\tau + \int_{\mu-T_s}^{\mu} f_{\hat{T}_i}(\tau)\mathrm{d}\tau \\
&\quad + \int_{\mu}^{\mu+T_s} f_{\hat{T}_i}(\tau)\mathrm{d}\tau + \int_{\mu+T_s}^{t} f_{\hat{T}_i}(\tau)\mathrm{d}\tau
\end{aligned}$$

Solving the above integrals by substituting the appropriate PDFs derived for Case 1, Case 2, Case 3 and Case 4 in Section 11 and combining them, we get,

$$\begin{aligned}
F_{\hat{T}_i}(t) = \frac{1}{2(2-\alpha)(\alpha-1)^2T_s^2}\Bigg[&2T_s^2\Bigg(-\left(\frac{\lambda+t-T_s-\mu}{\lambda}\right)^{-\alpha} \\
&- \left(\frac{\lambda+t+T_s-\mu}{\lambda}\right)^{-\alpha} + \alpha\Bigg(\left(\frac{\lambda+t-T_s-\mu}{\lambda}\right)^{-\alpha} \\
&+ \left(\frac{\lambda+t+T_s-\mu}{\lambda}\right)^{-\alpha} - (\alpha-4)\alpha - 5\Bigg) + 2\Bigg) \\
&+ 4(\alpha-1)T_s(\lambda+t-\mu)\Bigg(\left(\frac{\lambda+t+T_s-\mu}{\lambda}\right)^{-\alpha} \\
&- \left(\frac{\lambda+t-T_s-\mu}{\lambda}\right)^{-\alpha}\Bigg) + 2(\alpha-1)(\lambda+t-\mu)^2 \\
&\times\Bigg(\left(\frac{\lambda+t-T_s-\mu}{\lambda}\right)^{-\alpha} + \left(\frac{\lambda+t+T_s-\mu}{l}\right)^{-\alpha} \\
&- 2\left(\frac{\lambda+t-\mu}{\lambda}\right)^{-\alpha}\Bigg)\Bigg]
\end{aligned}$$

References

1. J. Lundén, V. Koivunen, and H. V. Poor, "Spectrum Exploration and Exploitation for Cognitive Radio: Recent Advances," *IEEE Signal Processing Magazine*, vol. 32, no. 3, pp. 123–140, 2015.
2. M. Cardenas-juarez, M. A. Diaz-ibarra, U. Pineda-rico, A. Arce, and E. Stevens-navarro, "On Spectrum Occupancy Measurements at 2 . 4 GHz ISM Band for Cognitive Radio Applications," *International Conference on Electronics, Communications and Computers*, pp. 25–31, 2016.
3. J. Eze, S. Zhang, E. Liu, and E. Eze, "Cognitive radio technology assisted vehicular ad-hoc networks (vanets): Current status, challenges, and research trends," in *2017 23rd International Conference on Automation and Computing (ICAC)*, Sep. 2017, pp. 1–6.
4. Y. C. Liang, K. C. Chen, G. Y. Li, and P. Mähönen, "Cognitive radio networking and communications: An overview," *IEEE Trans. Veh. Technol.*, vol. 60, no. 7, pp. 3386–3407, 2011.
5. H. Urkowitz, "Energy detection of unknown deterministic signals," *Proc. IEEE*, vol. 55, no. 4, pp. 523–531, 1967.
6. Y. Chen and H. S. Oh, "A survey of measurement-based spectrum occupancy modeling for cognitive radios," *IEEE Communications Surveys and Tutorials*, vol. 18, no. 1, pp. 848–859, 2016.
7. F. F. Digham, M. S. Alouini, and M. K. Simon, "On the energy detection of unknown signals over fading channels," *IEEE Trans. Commun.*, vol. 55, no. 1, pp. 21–24, Jan 2007.
8. H. Ahmadi, Yong Huat Chew, Pak Kay Tang, and Y. A. Nijsure, "Predictive opportunistic spectrum access using learning based hidden markov models," in *Proc. PIMRC*, Sep. 2011, pp. 401–405.
9. H. Ahmadi, I. Macaluso, and L. A. DaSilva, "The effect of the spectrum opportunities diversity on opportunistic access," in *IEEE International Conference on Communications (ICC)*, June 2013, pp. 2829–2834.
10. I. Macaluso, H. Ahmadi, and L. A. DaSilva, "Fungible orthogonal channel sets for multi-user exploitation of spectrum," *IEEE Trans. Wireless Commun.*, vol. 14, no. 4, pp. 2281–2293, April 2015.
11. Y. Liu and A. Tewfik, "Hyperexponential approximation of channel idle time distribution with implication to secondary transmission strategy," in *Proc. IEEE ICC*, June 2012, pp. 1800–1804.
12. C. Liu, P. Pawelczak, and D. Cabric, "Primary user traffic classification in dynamic spectrum access networks," *IEEE J. Sel. Areas Commun.*, vol. 32, no. 11, pp. 2237–2251, November 2014.
13. Y. Shabara, A. H. Zahran, and T. ElBatt, "Efficient spectrum access strategies for cognitive networks with general idle time statistics," in *Proc. IEEE ICC*, June 2015, pp. 7743–7749.
14. A. Agarwal, S. Dubey, M. A. Khan, R. Gangopadhyay, and S. Debnath, "Learning based primary user activity prediction in cognitive radio networks for efficient dynamic spectrum access," in *Proc. SPCOM*, June 2016, pp. 1–5.
15. A. Al-Tahmeesschi, M. Lopez-Benitez, J. Lehtomaki, and K. Umebayashi, "Investigating the estimation of primary occupancy patterns under imperfect spectrum sensing," in *Proc. IEEE WCNC*, March 2017, pp. 1–6.
16. A. Al-Tahmeesschi, M. López-Benítez, K. Umebayashi, and J. Lehtomäki, "Analytical study on the estimation of primary activity distribution based on spectrum sensing," in *Proc. IEEE PIMRC*, Oct 2017, pp. 1–5.
17. A. Al-Tahmeesschi, M. López-Benítez, J. Lehtomäki, and K. Umebayashi, "Accurate estimation of primary user traffic based on periodic spectrum sensing," in *Proc. IEEE WCNC*, April 2018, pp. 1–6.
18. A. Al-Tahmeesschi, M. López-Benítez, J. Lehtomäki, and K. Umebayashi, "Improving primary statistics prediction under imperfect spectrum sensing," in *Proc. IEEE WCNC*, April 2018, pp. 1–6.
19. M. López-Benítez and F. Casadevall, "Time-dimension models of spectrum usage for the analysis, design, and simulation of cognitive radio networks," *IEEE Trans. Veh. Technol.*, vol. 62, no. 5, pp. 2091–2104, 2013.
20. R. J. Larsen, M. L. Marx *et al.*, *An introduction to mathematical statistics and its applications*. Prentice-Hall Englewood Cliffs, NJ, 1986, vol. 2.
21. M. López-Benítez and F. Casadevall, "Modeling and simulation of time-correlation properties of spectrum use in cognitive radio," in *6th International ICST Conference on Cognitive Radio Oriented Wireless Networks and Communications (CROWNCOM)*, June 2011, pp. 326–330.
22. N. L. Johnson, S. Kotz, and N. Balakrishnan, "Continuous univariate distributions, vol. 2 of wiley series in probability and mathematical statistics: applied probability and statistics," 1995.
23. W. H. Press, S. A. Teukolsky, W. T. Vetterling, and B. P. Flannery, *Numerical recipes 3rd edition: The art of scientific computing*. Cambridge university press Cambridge, 2007, vol. 3.
24. D. Zwillinger, *"Table of Integrals, Series, and Products", Eighth Edition*, 2014.
25. W. R. Inc., "Mathematica online, Version 11.3," champaign, IL, 2018.
26. M. López-Benítez, F. Casadevall, A. Umbert, J. Pérez-Romero, R. Hachemani, J. Palicot, and C. Moy, "Spectral occupation measurements and blind standard recognition sensor for cognitive radio networks," in *Proc. IEEE CROWNCOM*, 2009, pp. 1–9.
27. X. Chu, D. Lopez-Perez, Y. Yang, and F. Gunnarsson, *Heterogeneous Cellular Networks: Theory, Simulation and Deployment*. Cambridge University Press, 2013.